Applied Thermal Engineering 279 (2025) 127633

Contents lists available at ScienceDirect

Applied Thermal Engineering

journal homepage: www.elsevier.com/locate/apthermeng

Research Paper

CFD analysis of multi-layer cooling channels in three-dimensionally structured grinding wheels

Sharlane Costa [a,b,c], Paulina Capela [a,d], Amauri Hassui [e], João Ribeiro [c,*], Mário Pereira [f], Delfim Soares [a,b]

[a] CMEMS - Center for MicroElectromechanical, University of Minho, 4800-058 Guimarães, Portugal
[b] LABBELS – Associate Laboratory, Braga/Guimarães, Portugal
[c] CIMO - Mountain Research Center, Braganca, Portugal
[d] MEtRICs, Mechanical Eng. Dep., Univ. of Minho, Campus de Azurém, Guimarães, Portugal
[e] Department of Manufacturing and Materials Engineering, School of Mechanical Engineering, University of Campinas – UNICAMP, 13083-860 Campinas, São Paulo, Brazil
[f] Centro de Física das, Universidades do Minho e do Porto, Braga, Portugal

ARTICLE INFO

Keywords:
Taguchi method
Grinding performance
Grinding
CFD
Thermal control
Fluid distribution
Structured grinding wheel

ABSTRACT

Minimizing heat damage and surface integrity loss in grinding depends on effective cooling. Conventional techniques, however, suffer with low efficiency because of the fast air barrier restricting fluid access. Grinding wheels with internal cooling channels have been suggested to solve this; nonetheless, the impact of channel geometry and multi-layer topologies is yet unknown. This work investigates their effects on coolant flow pattern and thermal performance by means of computational fluid dynamics (CFD) simulations, experimental validation, and statistical optimization combined. The ideal arrangement was found by the Taguchi- Grey study to be 30 channels, 78° inclination, 1.7 mm diameter and 2 mm interlayer distance. ANOVA determined that diameter (59.7 %) and number of channels (21.8 %) are the most influential parameters. CFD results showed that multilayer structures significantly increase fluid dispersion in the workpiece. The three-layer design stood out for providing the most uniform and dynamic fluid distribution, reducing cooling inconsistencies. Grinding tests confirmed that this configuration achieved the lowest temperatures for all different depths of cut. These findings highlight that increasing the number of flutes alone is insufficient; a three-dimensional flute structure with optimized geometry is essential to ensure efficient cooling. By integrating numerical modeling, statistical optimization, and experimental validation, this study provides a framework for designing grinding wheels with internal cooling channels, improving fluid distribution and thermal control.

1. Introduction

The quality of the surface finish in grinding processes is a major concern for manufacturing industries due to the high temperatures generated in the grinding zone [1]. The temperature of the workpiece's surface can reach extremely high levels and, under particularly severe conditions, may exceed 1000 °C [2]. Such extreme temperatures can cause adverse structural changes, including phase transformations and residual stress generation. Among the most common grinding-induced defects in the workpiece surface layer are burning, metallurgical phase transformations, softening (tempering) with possible rehardening, tensile residual tensile stresses, cracks, and reduced fatigue strength [3,4].

Different cooling and lubrication techniques are used in grinding to reduce these problems; the most often used one is flood cooling, in which the grinding zone receives significant coolant application [5]. But since an air barrier around the high-speed spinning wheel causes over 60 % of the fluid to not reach the grinding zone [6–8], flood cooling is generally ineffective.

To raise lubrication efficiency, substitutes as nano-MQL and minimum quantity lubrication (MQL) have been investigated [9]. While nano-MQL improves this process by suspending nanoparticles in the fluid, hence enhancing thermal conductivity and lubricating efficiency [10]. MQL substantially reduces fluid consumption by spraying a tiny mist of cooling fluid immediately to the grinding interface. MQL has

* Corresponding author.
E-mail addresses: scosta@dem.uminho.pt (S. Costa), pcapela@dem.uminho.pt (P. Capela), hassui@fem.unicamp.br (A. Hassui), jribeiro@ipb.pt (J. Ribeiro), mpereira@fisica.uminho.pt (M. Pereira), dsoares@dem.uminho.pt (D. Soares).

https://doi.org/10.1016/j.applthermaleng.2025.127633
Received 9 May 2025; Received in revised form 11 July 2025; Accepted 20 July 2025
Available online 22 July 2025

several limitations, especially in high-speed grinding applications where the amount of fluid would not be sufficient to provide appropriate cooling, resulting in greater surface temperatures and potentially thermal damage to the workpiece. Furthermore, MQL could prove less successful when machining materials with poor machinability, such as superalloys, since the high-speed air barrier created around the wheel may make it difficult to adequately penetrate the grinding zone [11]. Moreover, MQL can cause clogging of the grinding wheel pores due to lubricant and debris accumulation inside the porous structure, so compromising the grinding performance and raising the wheel loading risk [12,13].

Furthermore, the use of traditional coolant fluids presents environmental and economic concerns. Excessive use of cutting fluids not only increases production costs but also raises environmental and health risks due to the disposal of used fluids, which often contain harmful chemicals [14,15]. Consequently, developing more effective fluid delivery techniques that reduce the volume of fluid applied while preserving or enhancing cooling performance attracts increasing attention [11,16].

Recent innovations in grinding tools, such as the development of textured grinding wheels, have aimed to solve these difficulties by optimizing coolant distribution and enhancing energy economy. By up to 105 °C, textured wheels have been demonstrated to lower grinding zone temperatures and reduced cutting fluid usage by 60 % [8]. Using wheels with internal cooling channels, which provide direct fluid delivery to the grinding zone and thereby improve both cooling and lubricating performance [17–19], may be particularly beneficial in operations with restricted fluid access, such as internal grinding of bearing rings or cylinder liners. These internal channels offer a more focused, effective, and lasting cooling strategy, overcoming the limitations of external fluid application.

Computational Fluid Dynamics (CFD) provides a non-invasive and cost-effective approach to study fluid behavior in high-speed grinding environments, where direct measurement is challenging due to extreme temperatures and fast wheel rotation. Furthermore, CFD simulations facilitate the investigation of fluid behavior and heat dissipation mechanisms, which would be difficult to replicate in physical experiments [18,20].

Although several simulation studies have investigated the geometric parameters of surface-textured grinding wheels [21], the use of grinding wheels with an internal network of cooling channels remains a relatively new approach [22–24]. However, the influence of internal geometry, such as the number, arrangement, and diameter of channels, on fluid flow and thermal performance has not been systematically evaluated. This study addresses this gap by combining Computational Fluid Dynamics simulations, experimental validation and statistical optimization, using the Taguchi method to improve coolant distribution in grinding processes.

This integrated approach provides a comprehensive evaluation of how internal cooling channel geometries influence fluid flow, cooling efficiency, and thermal performance. CFD simulations allow for a detailed analysis of fluid behavior, while the Taguchi method systematically identifies the most influential geometric parameters affecting cooling efficiency. Additionally, experimental validation was conducted using customized grinding wheels with optimized internal channels, assessing their real-world thermal performance under different operating conditions. By bridging the gap between numerical modeling and practical application, this study establishes a systematic framework for optimizing grinding wheel design, ultimately enhancing cooling efficiency, reducing thermal damage and improving surface quality in grinding operations.

2. Materials and methods

2.1. Experimental design and factor selection using the Taguchi method

To optimize the factors influencing fluid distribution in the grinding system and minimize the number of simulations, the Taguchi method was employed. This method is widely applied in experimental and numerical studies involving multiple control variables. Its main benefit comes from its efficiency in lowering the combinations of levels and factors of interest using an orthogonal array [25,26]. In this study, the L18 array was used because it is suitable for five factors, each with three levels, allowing for the evaluation of interactions with a minimal number of simulations. The selected variables and their levels are presented in Table 1.

These factors were selected due to their potential influence on the transport and distribution of coolant fluid during the grinding process, considering the geometric dimensions of the abrasive grinding wheels. Fig. 1 illustrates some examples of the geometries used in the simulations, which aid in understanding the geometric parameters studied:

- **Number of Channel Layers:** The abrasive wheel can be configured with one (Fig. 1a), two (Fig. 1b-c), or three layers of channels. For configurations with two layers, the channels are positioned alternately (Fig. 1b). In the case of three layers, the two outer layers are aligned, while the middle layer is staggered (Fig. 1d). This configuration results in a dynamic cooling process with two possible situations during operation: one, where only one channel comes into contact with the workpiece (Fig. 1d), and another, where the two outer channels make simultaneous contact (Fig. 1e). For the experiments with three layers, simulations were conducted for both scenarios, and the average of the results was used to assess geometry cooling efficiency.
- **Number of Channels:** This is the total of channels in the tridimensional grinding wheel. Since additional departure points increase coverage, the inclusion of more channels aims to enhance the homogeneity of cooling fluid allocation over the workpiece. But as the number of channels rises, the fluid volume per channel drops, which might cause the flow rate inside every channel to drop as well. Three levels of study were 18, 24, and 30 channels. Fig. 1a provides a 24-channel design example.
- **Channel Inclination (θ):** The channel inclination refers to the angle between the channels and the workpiece, as shown in Fig. 1a; when the angle is 90°, the channels are perpendicular to the workpiece surface. Smaller angles (83° and 78°) slant the channels towards the workpiece, therefore guiding the fluid in a more tangential direction—expected to increase fluid penetration at the workpiece contact.
- **Channel Diameter:** The channel diameter directly influences fluid flow through the system. Larger diameters offer less resistance to flow, allowing the fluid to move more easily through the system, while smaller diameters (1 mm) increase fluid velocity, which may enhance penetration at the contact interfaces. The analysis was conducted for three diameter levels: 1 mm, 1.5 mm, and 1.7 mm.
- **Interlayer Distance (ID):** Denoted as “ID” in Fig. 1c, the interlayer distance controls the distance between channel layers within the abrasive wheel. Three levels of this variable were chosen for this study: 1 mm, 1.5 mm, and 2 mm. While bigger gaps allow for a more uniform flow of the fluid, lower interlayer distances result in closer proximity of the channels, therefore perhaps concentrating the fluid in particular places. There are no extra layers to be spaced, hence in

Table 1
Factors and their levels, used in the Taguchi experimental design.

Factors		Levels			
1	Number of Channel Layers	1	2	3	–
2	Number of Channels	18	24	30	–
3	Inclination – θ (deg)	90	83	78	–
4	Channel diameter (mm)	1	1.5	1.7	–
5	Interlayer Distance – ID (mm)	0	1	1.5	2

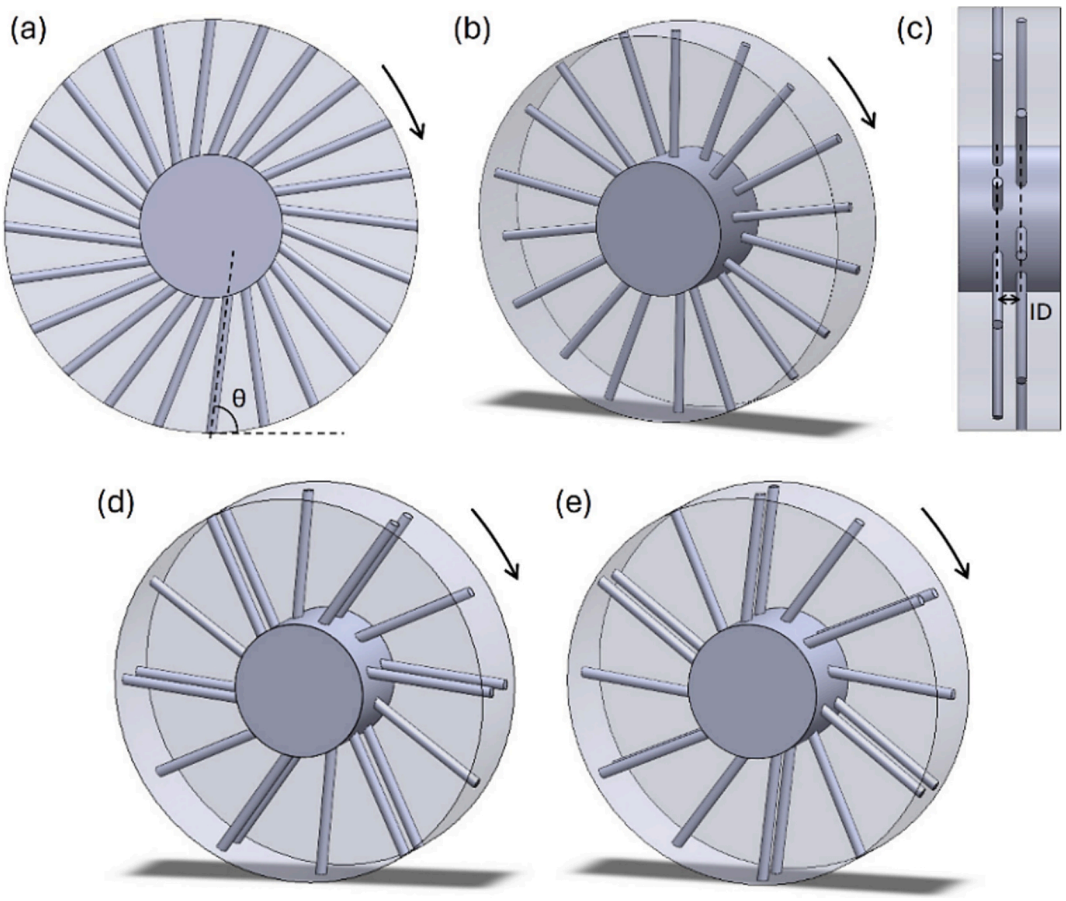

Fig. 1. Front view of a single-layer grinding wheel with channels inclined at an angle θ relative to the workpiece surface (a), structured grinding wheels with two layers of channels (b), side view showing the interlayer distance (ID) (c), and three-layer configurations in two scenarios: one channel in contact with the workpiece (d) and two channels in contact with the workpiece (e).

cases with a single layer the interlayer distance is regarded as 0 in the orthogonal matrix.

The geometries assessed in this work were chosen depending on the Taguchi L18 orthogonal array to guarantee an effective investigation of important design criteria and reduce computational effort. Table 2 lists the factor levels together with their matching simulations.

Table 2
Geometry factor combinations used in the simulations according to the Taguchi experimental design (L18 array).

Geometry	Number of Layers	Number of Channels	Inclination (deg)	Channel Diameter (mm)	Interlayer Distance (mm)
1	1	18	90	1	0
2	1	24	83	1.5	0
3	1	30	78	1.7	0
4	2	18	90	1.5	2
5	2	24	83	1.7	1
6	2	30	78	1	1.5
7	3	18	83	1.7	1.5
8	3	24	78	1	2
9	3	30	90	1.5	1
10	1	18	83	1	0
11	1	24	78	1.5	0
12	1	30	90	1.7	0
13	2	18	78	1.7	1
14	2	24	90	1	1.5
15	2	30	83	1.5	2
16	3	18	78	1.5	1.5
17	3	24	90	1.7	2
18	3	30	83	1	1

2.2. Geometric model and setup

The geometric model consists of a structured abrasive wheel with internal cooling channels, positioned above the workpiece. The coolant is supplied through the central axis of the wheel, distributing itself through the internal channels until it reaches the contact surface with the workpiece. To analyze how the fluid mixes with the air and spreads across the workpiece, a control volume box was created around the wheel. This box represents the environment around the wheel, allowing for the analysis of fluid dispersion. Its open walls maintain atmospheric pressure, serving as outlets for the fluid, as shown in Fig. 2. Additionally, Fig. 2 highlights the wheel's rotation direction, which plays a key role in fluid dispersion and distribution in the contact zone.

The grinding wheel has a diameter of 62 mm, with a center bore of 21 mm in diameter and a width of 15 mm, as shown in Fig. 3. The wheel is attached to a 12 mm diameter shaft, through which the coolant is introduced. Before the fluid is directed into the channels, the wheel's central bore serves as a temporary reservoir. The center of the wheel aligns with the Z-axis, which is defined as the axis of rotation. The geometric model was created and imported into ANSYS for CFD simulations, allowing the analysis of coolant flow pattern across different channel configurations and operating conditions.

A minimum distance of 1 mm was defined between the wheel and the workpiece to facilitate mesh generation and ensure numerical stability, especially due to the complexity of the rotating multi-channel geometry. This modeling approach has also been adopted in previous studies on grinding wheel flow simulations [27]. It is worth noting that

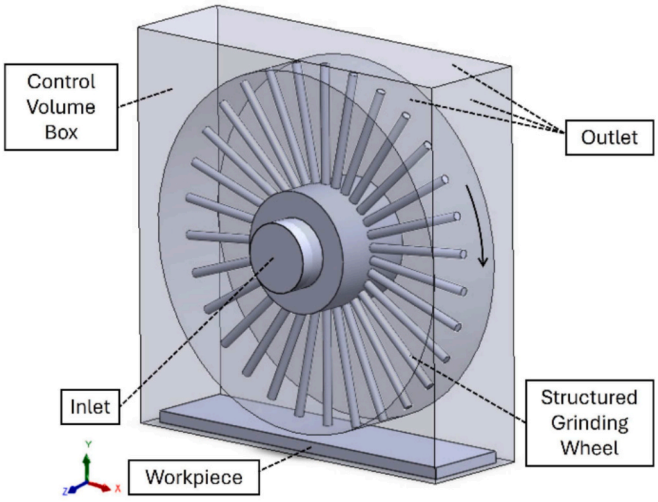

Fig. 2. Grinding wheel and fluid domain model.

the purpose of the simulation is to evaluate coolant distribution in the vicinity of the contact zone, not the mechanical interaction between the tool and the workpiece.

The quality of the mesh for CFD simulations was evaluated through a convergence test, where the number of elements was varied to ensure the accuracy of the results. The convergence criterion used was the mass flow rate of water in the contact region between the grinding wheel and the workpiece. The mesh independence study was performed for geometry 1, corresponding to the first experiment in the Taguchi array (Table 2).

Polyhedral elements discretized the computational domain; following the convergence study, a mesh with about 3 million elements was chosen as the best configuration. From this number of elements forward, the mass flow rate stabilizes according to the graph in Fig. 4, therefore verifying the sufficient refinement of the mesh for correct findings. This configuration contained around 3.3 million nodes, with an element size of 0.1 mm in the internal cooling channels and grinding zone, 0.4 mm in the control volume surrounding the wheel, and 0.5 mm in the center of the grinding wheel and the fluid inlet region. Choosing this mesh allowed one to strike a compromise between computational efficiency and solution correctness, thereby assuring that the simulation faithfully records the main fluid-dynamic interactions in the cooling system within realistic computational expenses.

The abrasive wheel was handled as a solid without porosity, and the water was employed as the cooling fluid instead of a more complicated, multi-component coolant, so simplifying certain computing resources without affecting the accuracy of the results. These simplifications free the model from the additional complexity of material features like porosity or chemical composition of the fluid enabling focus on the interaction between the coolant and the workpiece.

ANSYS was used in multiphase modeling to investigate fluid distribution on the workpiece. Since simulations include two immiscible phases—air and water—the Volume of Fluid (VOF) model was chosen since it is appropriate. VOF was used because it could precisely depict the interface between both phases, therefore allowing a correct evaluation of the fluid reaching the workpiece surface [28]. The aim is to assess the fluid flow through the internal channels of the wheel, reach the work surface, and distribute, therefore offering information on the effectiveness of the cooling system.

In the VOF model, the Implicit configuration was chosen to enhance numerical stability and reduce processing time, as this method solves the

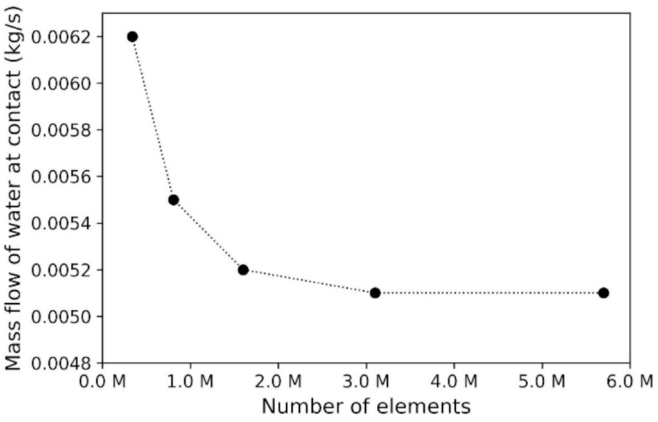

Fig. 4. Mesh convergence test results — Relationship between the number of elements and the mass flow rate of water at the contact surface between the grinding wheel and the workpiece.

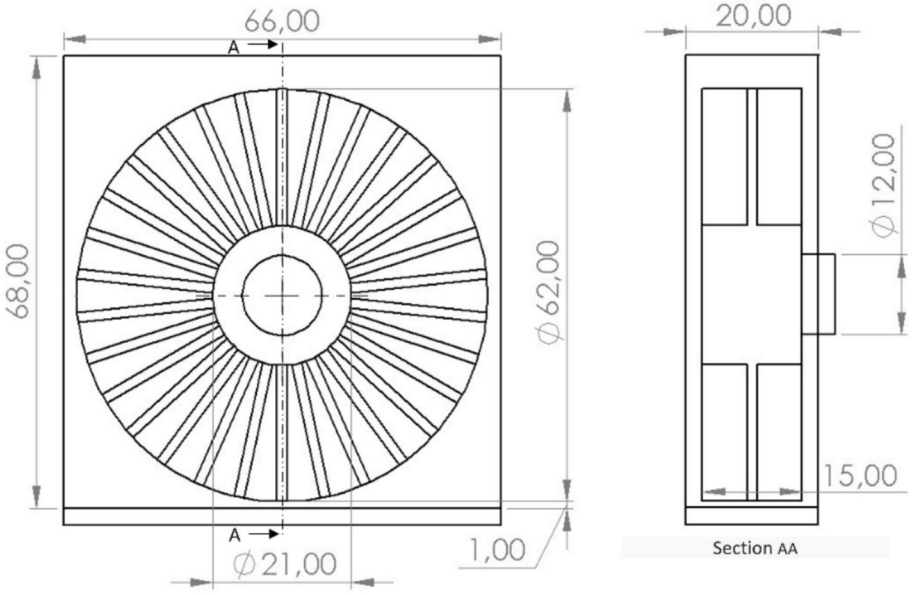

Fig. 3. Dimensional drawing of the structured grinding wheel used in simulations.

fluid equations simultaneously at each time step [29,30]. To control the phase mixture, the dispersed option was turned on whereby the coolant (water) is distributed inside the continuous phase (air) [31]. The surface tension between air and water correlates with the phase interaction value, 0.0728 N/m [32]. Essential for the proper interaction between the phases, this value is derived from the physical characteristics of the simulated system. Considered as acting toward the workpiece, gravity affected the fluid's behavior.

Widely employed for turbulent flows in industrial applications including flow around solid surfaces and fluid jets, the k-ε (2 eqn) realizable model was the turbulence model chosen [24,27]. The realizable version was chosen for its robustness in improving the accuracy of highly distorted flows, such as those occurring in the interaction between the coolant and the workpiece [33,34].

To simulate the rotation of the abrasive wheel, the Multiple Reference Frame (MRF) method was used, as appropriate for steady-state simulations, thus avoiding the need for transient simulation [35,36]. The griding wheel was set to rotate at 2000 rpm, with the center defined as the rotating zone. The rotating internal surfaces (channels and shaft) were treated as rotating zones relative to the wheel's center.

The boundary conditions included specifying the fluid inflow as a mass flow inlet with a flow rate of 0.0499 kg/s of water, therefore matching 3 L/min. This is the coolant arriving via the wheel's center shaft. Setting the outlet as a pressure outlet, free flow from the control zone under atmospheric pressure could be allowed. To guarantee that the shaft, center, and abrasive wheel areas were completely filled with water from the beginning of the simulation, the volume fraction in these areas was set to 1 during initialization, therefore helping to attain simulation convergence.

Appropriate for simultaneous solution of pressure and velocity fields, the numerical scheme used was Coupled with the Volume Fractions option active [37]. The stability of the model was guaranteed over the simulation by a set global time step [29].

The main setup configurations are summarized in Table 3.

In the post-processing conducted with ANSYS, data on mass flow rate and water volume fraction were collected. To measure the mass flow rate, a plane perpendicular to the grinding wheel at the contact line, referred to as the "contact plane," was created with dimensions of 1 mm in height (representing the distance between the grinding wheel and the workpiece) by 15 mm in width (wheel width). This plane allowed the determination of the mass flow rate of water passing through it.

To understand the water volume fraction curves, a line, referred as the "contact line", was drawn along the surface of the workpiece, centered relative to the wheel, as illustrated in Fig. 5a. This line's water volume fraction captures the water distribution profile in the contact zone. Calculating the area under the volume fraction curve allowed one to estimate the water content along this line. Together with the mass flow rate at the contact plane, this value was applied in the Grey correlation coefficient study. Fig. 5a illustrates this analysis for geometry 3, which corresponds to the one-layer configuration with 30 channels, a 78° inclination, and a 1.7 mm diameter. The corresponding water volume fraction curve along this line is presented in Fig. 5b.

Table 3
Key simulation setup configurations, including the VOF multiphase model, grinding wheel rotation settings, and boundary conditions for the cooling fluid.

Parameter	Configuration	
Multiphase Model	Volume Of Fluid (VOF): Implicit, Dispersed. Phase Interaction: 0.0728 N/m	
Fluid Properties [38]	Air	Water
	Density: 1.225 kg/m^3	Density: 998.2 kg/m^3
	Viscosity: 1.79 × 10^{-5} kg/(m.s)	Viscosity: 1.00 × 10^{-3} kg/(m.s)
Turbulence Model	k-epsilon (2 eqn); Realizable	
Rotation Method	Multiple Reference Frame (MRF); 2000 rpm	
Boundary Conditions	Inlet: Mass flow inlet (0,0499 kg/s of water) Outlet: *Pressure outlet*, free flow to the environment	
Numerical Scheme	Coupled with Volume Fractions activated	
Time Step Advancement	*Fixed global time step; steady-state*	
Gravity	Acting toward the workpiece	

To compute the Grey relational coefficients and Grey grades, the experimental responses were first normalized using the larger-is-better criterion, according to the equation [39]:

$$x_i' = \frac{x_i - \min(x_i)}{\max(x_i) - \min(x_i)} \tag{1}$$

After normalization, the Grey relational coefficient $\xi_i(k)$ was calculated for each response using:

$$\xi_i(k) = \frac{\Delta_{min} + \zeta.\Delta_{max}}{\Delta_i(k) + \zeta.\Delta_{max}} \tag{2}$$

where $\Delta_i(k)$ represents the absolute difference between the ideal normalized value (equal to 1) and the value of the i-th experiment for the k-th response. The distinguishing coefficient ζ was set to 0.5. Finally, the Grey relational grade γ_i was obtained by averaging the coefficients across the two considered responses (mass flow rate and water volume fraction), as shown below:

$$\gamma_i = \frac{1}{n}\sum_{k=1}^{n}\xi_i(k) \tag{3}$$

All calculations were implemented using Microsoft Excel based on the normalized output data obtained from CFD simulations.

2.3. Grinding tests

Under usual grinding settings, experimental validation was carried out to guarantee that the findings reflect actual industrial uses. Although the values might not be exactly like those used in the numerical simulations, the chosen conditions offer a consistent foundation for comparison, therefore enabling a good evaluation of the effect of cooling channel topologies on cooling efficiency. Moreover, the experimental tests evaluated the thermal performance of the wheels, as a complementary aspect.

The experimental validation was carried out using three "best" grinding wheels with optimized geometries to assess the impact of fluid channel arrangement on cooling efficiency during grinding. The wheels were manufactured through a pressing and sintering process, where a 3D organic structure was embedded in the green body to create internal fluid channels. During sintering, this structure was eliminated, leaving precisely formed channels inside of the final product [40].

The grinding parameters used in the experiments are presented in Table 4. For every experimental condition, the tests consisted of three repetitions. Prior to the grinding tests, the wheel was dressed using a multi-point diamond dresser at a rotation speed of 1000 rpm, a feed rate of 100 mm/min, and a dressing depth of 30 μm.

The temperature acquisition was carried out using a 1.5 mm diameter thermocouple, inserted into the workpiece 1 mm below the grinding wheel–workpiece contact surface, at a depth of 7.5 mm. By recording temperature readings at 0.2 s intervals, the data collecting device allowed constant observation of thermal fluctuations all through the operation. For each test, the maximum temperature recorded during the grinding cycle was considered for analysis.

Fig. 6 provides a detailed view of the grinding process, displaying the grinding wheel, worktable, and workpiece, along with the thermocouple position inside the workpiece. The directions of worktable feed (V_W) and grinding wheel rotation (V_S) are also indicated. The grinding machine was specifically designed with an internal cooling system [41], where the cutting fluid is injected through the central hole of the grinding wheel, ensuring its distribution through internal channels for local cooling and heat dissipation. The homogeneous distribution of the fluid

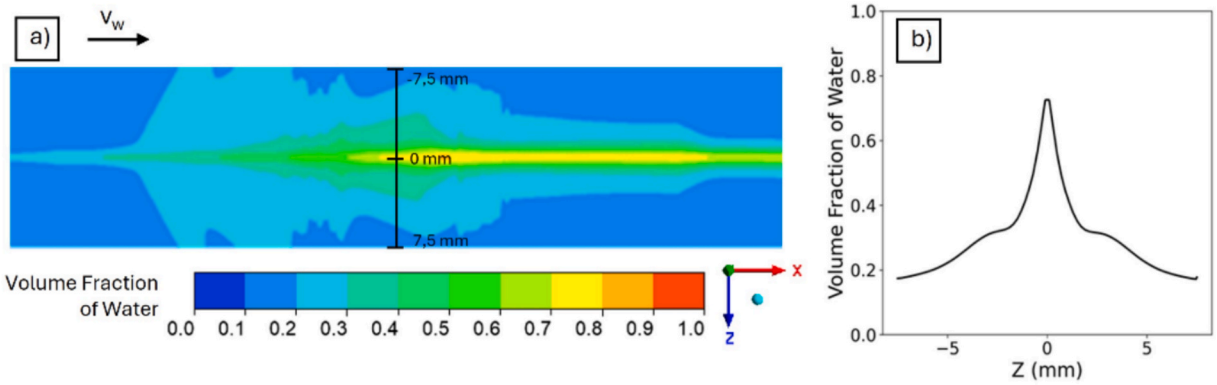

Fig. 5. Water Volume Fraction (a) on the surface of the workpiece and (b) along the contact line.

Table 4
Grinding parameters used in the experimental validation.

Grinding process parameters	Values
Grinding wheel rotation speed V_S (rpm)	5000
Workpiece feed rate V_W (mm/min)	100
Depth of cut (μm)	10, 20, 50, 80, 100, 120
Fluid flow rate	400 mL/min – distilled water
Grinding mode	Up Grinding
Grinding wheel abrasive	Alumina (Ø 62 × 16 × 21 mm)
Workpiece	AISI 1045 (80 × 15 × 10 mm)

through the channels is ensured by maintaining a continuous positive pressure in the internal chamber of the abrasive wheel.

3. Results and discussion

This section presents the results of the study in three stages: (i) optimization of cooling channel geometry using the Taguchi-Grey relational analysis, (ii) statistical evaluation of factor significance through ANOVA, and (iii) numerical and experimental validation of the optimized designs. The first section of the study determines the most important factors influencing cooling efficiency and cutting cooling fluid allocation; the second section calculates their statistical relevance. Comparing single-, two-, and three-layer arrangements using CFD models and experimental temperature data, the last section centers on fluid behavior dynamics.

3.1. Grey relational analysis

Grey Relational Analysis (GRA) was applied to evaluate system performance in terms of Mass Flow Rate and Volume Fraction (VF), considering five geometric parameters: Number of Layers, Number of Channels, Inclination, Diameter, and Interlayer distance. Table 5 presents the Grey relational coefficients and γ values (Grey relational grade) for each experiment. Higher γ values indicate better overall performance.

Experiment 3 achieved the highest γ value (0.889), indicating that this configuration had the best performance among all tested parameter combinations. The geometry for this experiment consisted of 1 layer, 30 channels, a 78° inclination, a 1.7 mm diameter, and an interlayer distance of 0 mm. This result suggests that this combination of parameters yields performance closest to the normalized ideal values for Mass Flow Rate and VF. However, other combinations, such as Experiments 15, 12, and 17, also demonstrated significant performance, with γ values of 0.753, 0.754, and 0.737, respectively.

While Experiment 3 showed the best individual performance, the Taguchi method was applied to determine the optimal levels for each geometric factor, optimizing the system in a more generalized manner, as shown in Table 6. Additionally, the effects of geometric parameters on Grey relational grades are presented in Fig. 7.

In Table 6, we observe that channel diameter and the number of channels have the greatest effect on the results, as indicated by the high delta values. The number of layers, however, appears inconsistent,

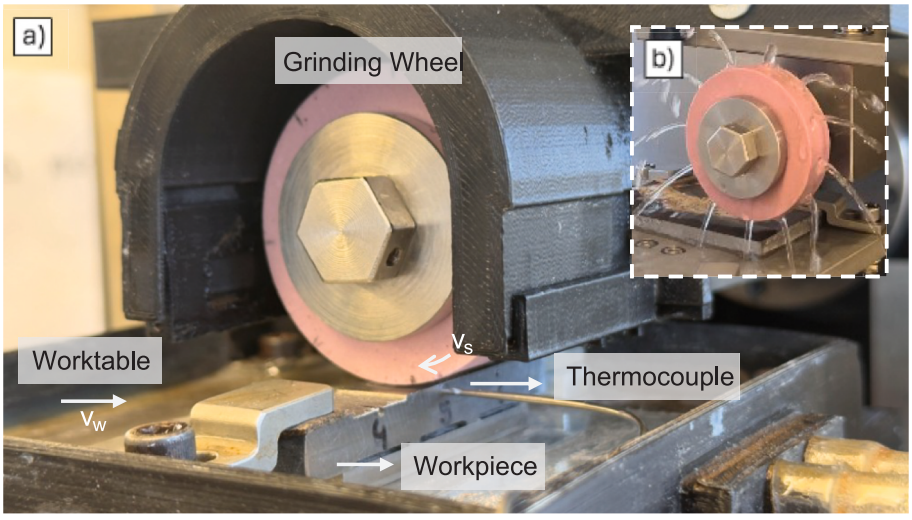

Fig. 6. Experimental grinding setup: (a) side view highlighting the grinding wheel, worktable, workpiece, and thermocouple position. Arrows indicate the directions of the grinding wheel rotation (Vs) and table feed (Vw); (b) frontal view detailing the fluid supply configuration for wheels with internal channels.

Table 5
Grey relational coefficient and Grey grade values.

No.	Grey relational coefficient		γ	Order
	Mass Flow Rate	VF		
1	0.345	0.333	0.339	18
2	0.558	0.658	0.608	8
3	**0.777**	**1.000**	**0.889**	**1**
4	0.548	0.411	0.479	13
5	0.744	0.548	0.646	6
6	0.459	0.404	0.432	15
7	0.738	0.356	0.547	10
8	0.590	0.458	0.524	12
9	0.817	0.386	0.602	9
10	0.333	0.351	0.342	17
11	0.548	0.677	0.612	7
12	0.678	0.829	0.754	**2**
13	0.626	0.451	0.538	11
14	0.452	0.381	0.417	16
15	0.899	0.608	0.753	**3**
16	0.922	0.381	0.652	5
17	1.000	0.473	0.737	**4**
18	0.552	0.364	0.458	14

showing the least effect among the factors analyzed. This could be attributed to the fact that the number of layers influences performance in a more indirect manner, primarily by affecting fluid distribution, which in turn impacts thermal control and chip removal capacity, factors that may not have been fully captured by the variables evaluated in the Grey Analysis.

As observed in Table 6 and Fig. 7, the optimal levels of geometric parameters for a three-dimensional channel structure, which maximize the Grey relational grade, are: Number of Layers = 1, Number of Channels = 3, Inclination = 3, Channel Diameter = 3, and Interlayer Distance = 4. This corresponds to a geometry with 1 layer, 30 channels, a 78° inclination, a 1.7 mm diameter, and 2 mm spacing between channels. However, when considering a single layer (Number of Layers = 1), the interlayer distance is no longer applicable. Thus, the optimized geometry corresponds to Experiment 3 in the Taguchi Orthogonal Table, which has already been tested, as it combines these factors without the need to assess interlayer distance, which does not apply to a single layer.

3.2. ANOVA analysis

The ANOVA table, presented in Table 7, was established to determine the contribution of each geometric parameter to the Grey relational grade. The degrees of freedom (df) represent the number of independent values that can vary for each factor, while the sum of squares (sum_sq) quantifies the total variation associated with each parameter. The mean square (mean_sq) is derived by dividing the sum of squares by the degrees of freedom, representing the average variability explained by each factor. The F-value compares the variability of each factor to the residual variability, where higher values indicate a stronger influence. Finally, the P-value assesses statistical significance, with values below 0.05 indicating that the factor has a real impact on the response rather than being a result of random variation.

Table 6
Main effects on Grey relation grades.

Level	Geometry Parameters				
	Number of Layers	Number of Channels	Inclination	Channel Diameter	Interlayer Distance
1	0.591	0.483	0.555	0.419	0.591
2	0.544	0.591	0.559	0.618	0.561
3	0.586	0.648	0.608	0.685	0.512
4	–	–	–	–	0.623
Delta	0.046	0.165	0.053	0.266	0.112
Order of effect	5	2	4	1	3

The ANOVA results confirm the Grey Relational Analysis findings, which identified channel diameter (59.7 %, P = 0.0006) and number of channels (21.8 %, P = 0.0110) as the most influential parameters for optimizing coolant flow pattern. Their statistical significance validates the observation that configurations with a larger channel diameter and more channels achieve superior mass flow rates and volume fraction distribution.

On the other hand, interlayer distance (5.5 %), inclination (2.7 %), and number of layers (2.1 %) had much lower contributions and were not statistically significant. This suggests a limited impact on cooling efficiency compared to channel diameter and number of channels. However, in a real grinding process, the contact between channels and the workpiece is dynamic, meaning that multi-layer configurations could still enhance fluid distribution over the complete grinding cycle. The staggered arrangement of multiple layers can promote a wider and equal distribution of the fluid, ensuring more uniform cooling under intermittent contact conditions.

To further investigate this effect, the next stage of the study evaluates the optimized parameters—30 channels, 78° inclination, 1.7 mm diameter, and 2 mm spacing—in one-, two- and three-layer configurations. This can provide a deeper understanding of the role of multiple layers in dynamic cooling fluid allocation and grinding efficiency.

3.3. Dynamic analysis of cutting fluid distribution

This section evaluates the fluid distribution across the workpiece for one-, two- and three-layer grinding wheel configurations. The analysis is performed dynamically over multiple time steps to assess how the fluid spreads across the contact surface, influencing cooling efficiency, chip removal and workpiece cooling. The objective is to understand how channel arrangement and motion impact the coverage and overall effectiveness of the cooling system.

For the single-layer configuration, the fluid distribution exhibits a well-defined central peak in water volume fraction along the contact line, as shown in Fig. 8(a). This indicates that most of the fluid is concentrated in the central region (i.e. near the outlet flow channel), while the peripheral areas receive significantly less cooling fluid. Since only one channel is active per cycle, there is minimal variation between time steps, meaning the fluid distribution remains relatively static over time (Fig. 8(c)).

As shown in Fig. 8(b), excess fluid accumulates in the central plane and is diverted to the environment, leading to substantial fluid waste. While this configuration ensures effective fluid distribution in the center, it provides limited coverage across the width of the contact line. This may reduce chip removal efficiency and increase the risk of thermal damage at the edges due to insufficient cooling.

In the two-layer configuration, the alternating arrangement of channels results in a more dispersed coolant flow pattern across the contact line, as seen in Fig. 9(a). The fluid is applied from different positions in successive time steps, leading to a cyclic pattern where the fluid peaks shift across the surface. Nonetheless, fluid concentration at the center of the contact line remains lower, even with the improvement over the single-layer configuration.

At time-step 1, channel C2 is positioned at the contact line (Fig. 9 (b)), located in the second layer (Z = 1.85 mm). However, the peak water concentration occurs at Z ≈ −2.5 mm, indicating that the fluid reaching the workpiece originates from channel C1 in the first layer, which has already passed the contact point; this occurs due to the rotation of the grinding wheel and the fluid pressure. As a result, the fluid released by earlier channels continues to cool the contact area, extending its coverage and reducing the heat accumulation in the regions near wheel-workpiece contact.

At time-step 2, C2 becomes the primary source of fluid in the contact zone, as shown by the peak at Z ≈ 2.0 mm in Fig. 9(a). This alternating

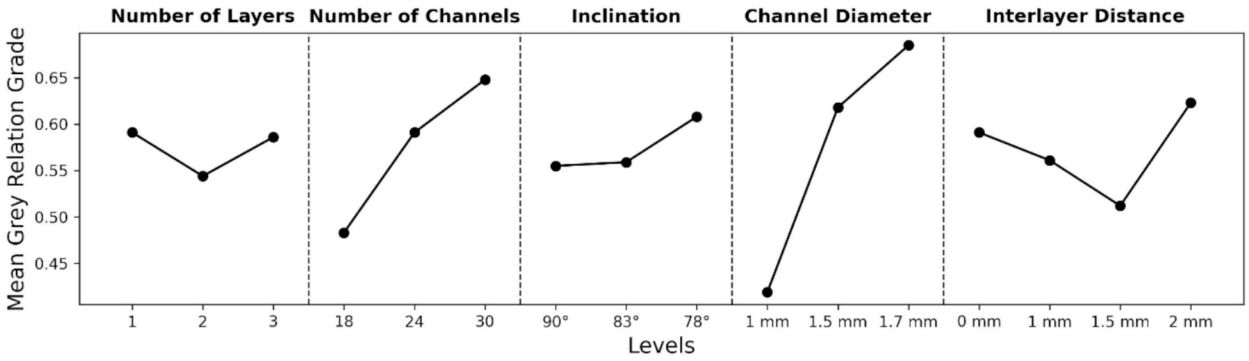

Fig. 7. Main effects plot for Mean Grey Relation Grade.

Table 7
Results of ANOVA on Grey relational grade.

	df	sum_sq	mean_sq	F-value	P-value	Influence
Number of Layers	2	0.0079	0.0040	0.8659	0.4613	2.1 %
Number of Channels	2	0.0841	0.0421	9.2069	0.0110	21.8 %
Inclination	2	0.0105	0.0052	1.1460	0.3711	2.7 %
Channel Diameter	2	0.2302	0.1151	25.1928	0.0006	59.7 %
Interlayer Distance	3	0.0212	0.0071	1.5464	0.2852	5.5 %
Residual	7	0.0320	0.0046			8.3 %

behavior repeats in time-step 3 and 4, mirroring previous time steps as the wheel rotates. The central region of the contact line retains a relatively stable fluid presence—never dropping below 20 %—but still exhibits lower overall intensity compared to surrounding areas (Fig. 9(c)).

Compared to the two-layer setup, the three-layer configuration (Fig. 10) introduces greater dynamism, with fluid application alternating effectively between time steps. A key observation is the cyclic flow movement along the contact line:

- At time step 1, the fluid concentration is higher at the sides, while the center is less cooled.
- At time step 2, the distribution shifts toward the center, reducing cooling at the sides.
- Time-step 3 redistributes the fluid again toward the sides, though with a different peak profile compared to step 1.
- Time-step 4 shows an asymmetric pattern, distinct from step 2, suggesting non-uniform yet continuous fluid movement.

This alternating pattern helps sustain cooling over time, avoiding dry spots and improving chip removal.

As in the previous configurations, a significant portion of the fluid

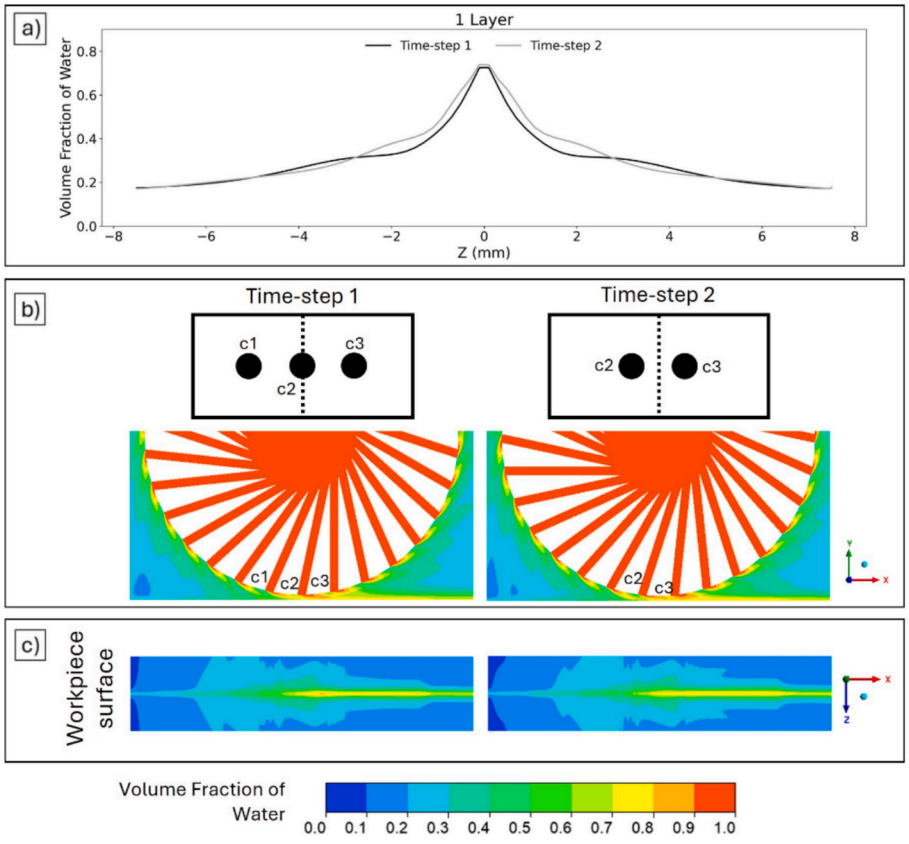

Fig. 8. Water volume fraction for the single-layer configuration over time: (a) along the contact line, (b) in each layer, and (c) on the workpiece surface.

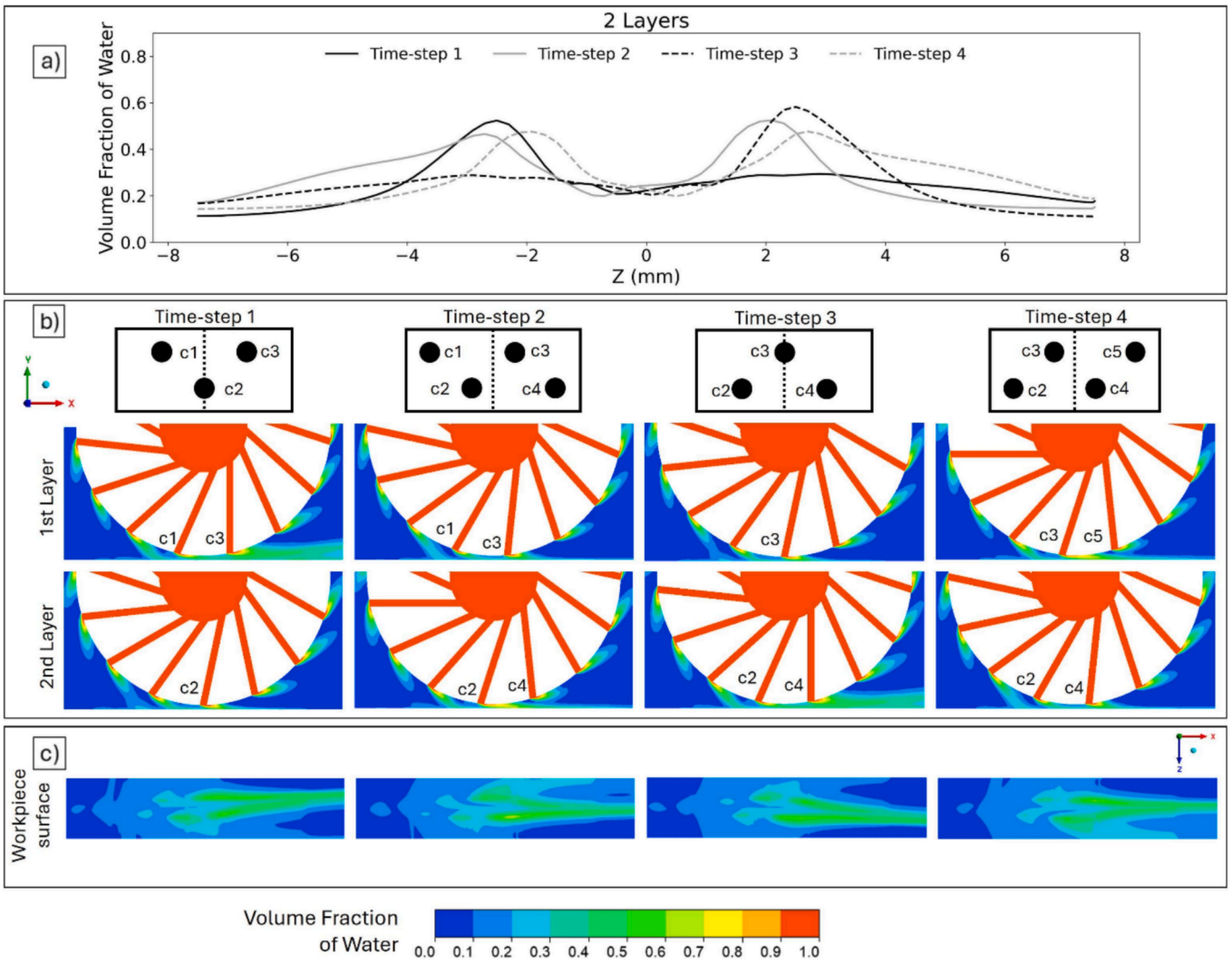

Fig. 9. Water volume fraction for the two-layer configuration over time: (a) along the contact line, (b) in each layer, and (c) on the workpiece surface.

reaching the contact line originates from channels that have already passed the contact point, due to the rotation of the grinding wheel. This effect is evident in Fig. 10(a) and Fig. 10(b), where the peaks in fluid concentration correspond to channels positioned ahead of the contact zone.

Furthermore, Fig. 10(b) shows that the central layer releases the most water, while the aligned lateral layers increase fluid replenishment, improving the overall efficiency of the cooling system. This more uniform fluid distribution minimizes waste and improves system performance.

A comparative analysis of the three configurations confirms that the three-layer setup provides the most effective and dynamic coolant flow pattern along the contact line. The alternating channels create a continuous cyclic flow, promoting more efficient debris removal and improved workpiece cooling. The two-layer configuration enhances fluid dispersion compared to the single-layer configuration, as the alternating channels distribute the fluid more evenly over a broader area; However, as discussed previously, this configuration still exhibits cooling gaps in the central zone where the contact line does not receive sufficient fluid potentially affecting the cooling performance in this region.

3.4. Experimental validation

In the experimental tests, the maximum temperature on the abrasive wheel/workpiece contact surface was recorded as a way of evaluating the cooling mechanism of the channel system introduced on the contact surface. These results were compared with the coolant distribution obtained in the numerical simulation. Fig. 11(a) presents the experimental results, showing the temperature variations for each configuration at different depths of cut. Additionally, Fig. 11(b, c, d) illustrate the grinding wheels used in the tests, highlighting the different channel arrangements for fluid distribution. The temperature values obtained are consistent with those reported in the literature for comparable grinding conditions [42].

The experimental results indicate that the three-layer configuration exhibited the lowest temperatures across all depths of cut. This behavior is attributed to enhanced fluid distribution, ensuring more efficient cooling and effective heat removal. The alternation of channels between layers promotes a continuous fluid flow, reducing the formation of dry regions at the grinding wheel–workpiece interface and improving thermal control, as shown in Fig. 10(a). This trend was also observed by Sieniawski et al, [19], who reported that the three-layer configuration enhances coolant delivery, reduces fluid waste and optimizes cooling efficiency in grinding operations.

The one- and two-layer configurations displayed very similar temperatures, both being significantly higher than the three-layer configuration. In the single-layer configuration, the fluid is more concentrated along the contact line, potentially improving cooling in the central region, although distribution in the lateral areas remains limited. The

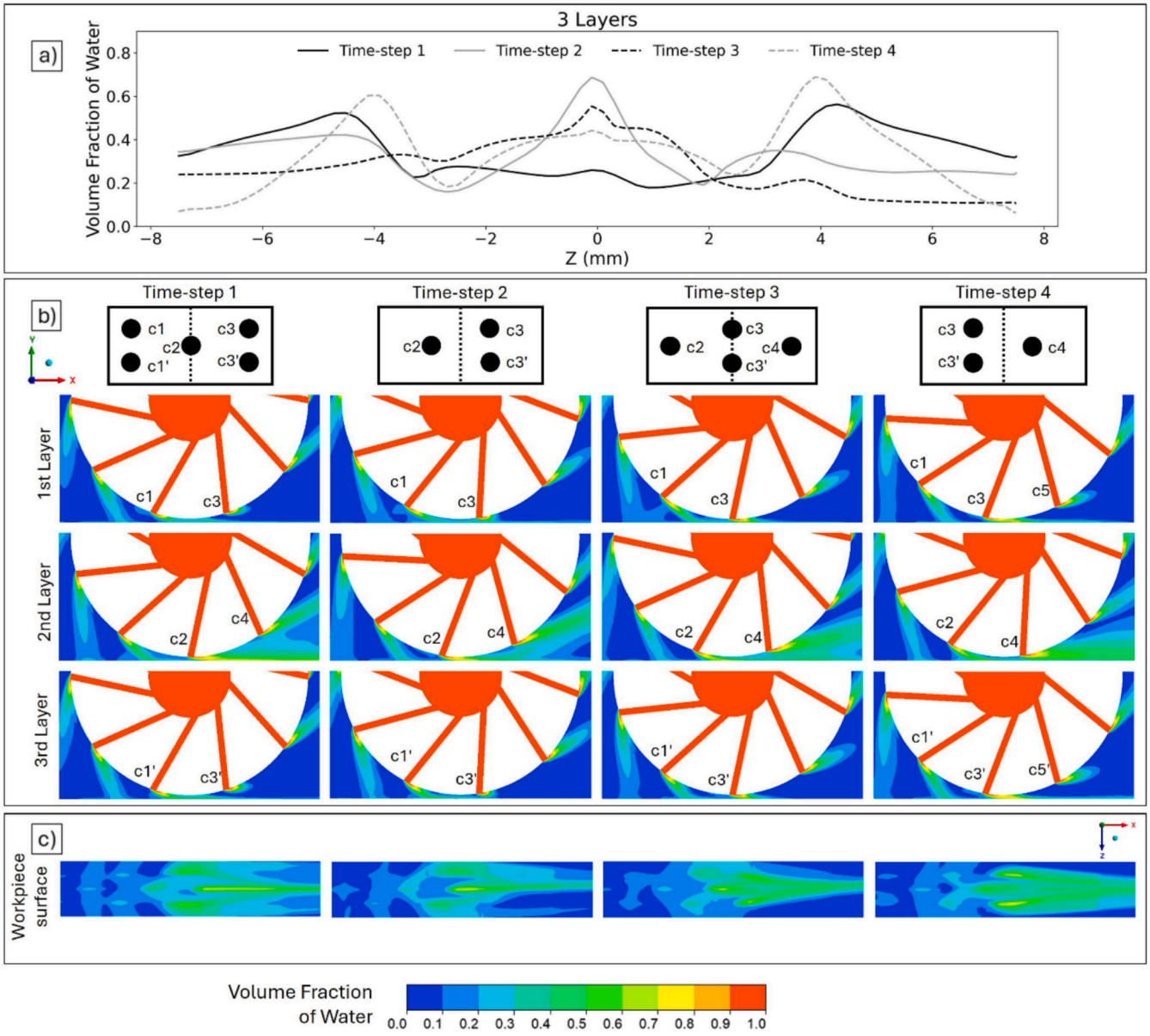

Fig. 10. Water volume fraction for the three-layer configuration over time: (a) along the contact line. (b) in each layer, and (c) on the workpiece surface.

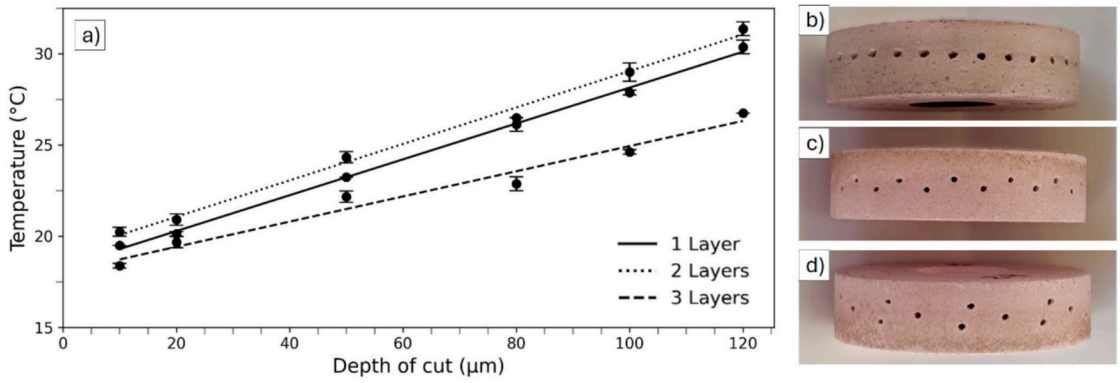

Fig. 11. (a) Maximum temperature as a function of depth of cut; (b–d) Grinding wheels with one, two, and three layers of channels, respectively.

simulations (Fig. 8(a)) confirm this behavior, showing that the single-layer configuration creates a well-defined fluid peak in the center, ensuring direct cooling at that location.

Meanwhile, the two-layer configuration showed a slightly higher temperature than the one-layer setup, which can be explained by less consistent coolant delivery at the interface due to channel alternation. As demonstrated in Fig. 9(a), the cooling pattern in the two-layer configuration is more dispersed, but gaps in central line are evident. These gaps may have resulted in localized deficient cooling, explaining the higher experimental temperatures. Additionally, the thermocouple position, located between the channels, may have contributed to this result, as the measurement was taken in a region with potentially reduced cooling, further reinforcing the findings from the simulations.

Another important aspect is the influence of cutting depth on the differences between configurations. As discussed in [2], in grinding processes, an increase in depth of cut results in higher thermal energy generation, intensifying the need for efficient heat dissipation to prevent thermal damage to the workpiece. This explains why, at low depths, temperature differences between configurations were minimal, whereas at higher depths, the three-layer configuration demonstrated significantly better performance. These results underscore the importance of an optimized cooling strategy under severe conditions to minimize thermal damage and preserve workpiece integrity.

While structural integrity was not the primary focus of this study, it is important to note that the highest channel density configuration tested (30 channels of 1.7 mm diameter) corresponds to only 2.3 % of the effective wheel surface. No signs of cracks or mechanical failure were observed during the grinding tests, indicating that the proposed design remained mechanically stable under the experimental conditions.

4. Conclusions

This study investigated the effect of internal cooling channels in grinding wheels, integrating Computational Fluid Dynamics (CFD), statistical optimization (Taguchi-Grey analysis) and experimental validation to evaluate fluid distribution and thermal performance. The following key conclusions were drawn:

- The Taguchi-Grey relational analysis identified the optimal channel configuration as 30 channels, a 78° inclination, a 1.7 mm diameter, and a 2 mm interlayer distance. Additionally, ANOVA determined that channel diameter (59.7 %) and number of channels (21.8 %) were the most influential parameters, confirming their critical role in optimizing fluid flow.
- The Grey Relational Analysis revealed that increasing the number of channels and their inclination angle positively influenced cooling performance. A higher number of channels improved fluid delivery, while greater inclination angles enhanced fluid penetration into the grinding zone, collectively optimizing the cooling efficiency.
- CFD simulations demonstrated that fluid dispersion improved with multi-layer configurations, but the two-layer setup exhibited gaps in central zone, leading to localized areas with lower fluid supply. The three-layer configuration, however, provided the most uniform and dynamic coolant flow pattern, ensuring cyclical replenishment of cooling fluid in the contact zone and mitigating cooling irregularities.
- The experimental results confirmed the superiority of the three-layer configuration, which consistently exhibited the lowest temperatures across all cutting conditions. The optimized multi-layer design enhanced cooling efficiency and reducing thermal accumulation, reinforcing the findings from CFD simulations.
- While a single-layer configuration concentrates cooling fluid at the center of the contact line, ensuring consistent cooling in that region, the two-layer setup disperses fluid more widely but creates gaps in the central zone. CFD simulations revealed that the staggered channels in the two-layer configuration caused alternating peaks in fluid distribution, leading to reduced concentration in some areas. Consequently, experimental validation showed that this setup resulted in higher temperatures than the single-layer configuration, highlighting the importance of ensuring continuous cooling in critical regions.
- The findings indicate that simply increasing the number of cooling channels is not sufficient; instead, a multi-layer design with an optimized geometry is essential to maximize cooling efficiency and minimize the fluid utilization. The three-layer configuration demonstrated superior thermal control, positioning it as a promising solution for enhancing grinding efficiency, extending tool lifespan, and ensuring superior workpiece quality.

CRediT authorship contribution statement

Sharlane Costa: Writing – review & editing, Writing – original draft, Visualization, Validation, Software, Methodology, Investigation, Formal analysis, Data curation. **Paulina Capela:** Writing – review & editing, Validation, Investigation, Formal analysis, Data curation. **Amauri Hassui:** Writing – review & editing, Validation, Formal analysis. **João Ribeiro:** Writing – review & editing, Supervision, Resources, Methodology, Investigation, Funding acquisition, Conceptualization. **Mário Pereira:** Writing – review & editing, Supervision, Methodology, Investigation, Formal analysis, Conceptualization. **Delfim Soares:** Writing – review & editing, Validation, Supervision, Resources, Project administration, Methodology, Funding acquisition, Formal analysis, Conceptualization.

Declaration of competing interest

The authors declare that they have no known competing financial interests or personal relationships that could have appeared to influence the work reported in this paper.

Acknowledgements

This work was supported by FCT national funds, under the national support to R&D units grant, through the reference project UIDB/04436. The authors are grateful to the Foundation for Science and Technology (FCT, Portugal) for financial support through national funds FCT/MCTES (PIDDAC) to CIMO (UIDB/00690/2020 and UIDP/00690/2020) and SusTEC (LA/P/0007/2020). This work is within the scope of Sharlane Costa Ph.D. degree, in progress, financially supported by the Portuguese Foundation for Science and Technology (FCT) through the Ph.D grant reference 2021.07352.BD.

Data availability

No data was used for the research described in the article.

References

[1] P.K. Gupta, N.P. Yadav, Computational investigation for structural behavior in deep grinding process, J. Braz. Soc. Mech. Sci. Eng. 45 (2023) 1–21, https://doi.org/10.1007/S40430-023-04201-1/FIGURES/30.
[2] P. Zhao, B. Lin, J. Zhou, B. Lv, J. Li, J. Zhang, L. Wang, T. Sui, Review of grinding temperature theory and measurement for the needs of the times: Promoting the development of advanced manufacturing, J. Mater. Process. Technol. 337 (2025) 118744, https://doi.org/10.1016/J.JMATPROTEC.2025.118744.
[3] W.B. Rowe, Temperatures in grinding-a review, J. Manufact. Sci. Eng. Trans. ASME 139 (2017), https://doi.org/10.1115/1.4036638/473165.
[4] S. Malkin, C. Guo, Thermal analysis of grinding, 56, (2), pp. 760-782 56 (2007) 760–782. Doi: 10.1016/j.cirp.2007.10.005.
[5] T. Tawakoli, B. Azarhoushang, Theoretical and experimental investigation of intermittent grinding of SiC with a segmented grinding wheel, Int. J. Abras. Technol. 4 (2011) 90–99, https://doi.org/10.1504/IJAT.2011.039005.
[6] W. Stachurski, J. Sawicki, K. Krupanek, K. Nadolny, Numerical analysis of coolant flow in the grinding zone, Int. J. Adv. Manuf. Technol. 104 (2019) 1999–2012, https://doi.org/10.1007/s00170-019-03966-x.

[7] W. Stachurski, R. Dębkowski, R. Rosik, R. Święcik, W. Pawłowski, Evaluation of the influence of the cooling method used during grinding on the operating properties of ceramic grinding wheels made with different abrasives, Adv. Sci. Technol. Res. J. 17 (2023) 1–18, https://doi.org/10.12913/22998624/162389.
[8] H.N. Li, D. Axinte, Textured grinding wheels: a review, Int. J. Mach. Tools Manuf. 109 (2016) 8–35, https://doi.org/10.1016/J.IJMACHTOOLS.2016.07.001.
[9] R.L. Rodriguez, J.C. Lopes, M.V. Garcia, F.S. Fonteque Ribeiro, A.E. Diniz, L. Eduardo de Ângelo Sanchez, H. José de Mello, P. Roberto de Aguiar, E. C. Bianchi, Application of hybrid eco-friendly MQL+WCJ technique in AISI 4340 steel grinding for cleaner and greener production, J Clean Prod 283 (2021) 124670, https://doi.org/10.1016/J.JCLEPRO.2020.124670.
[10] K. Kishore, S.R. Chauhan, M. Kumar Sinha, A comprehensive investigation on eco-benign grindability improvement of Inconel 625 using nano-MQL, Precis. Eng. 90 (2024) 81–95, https://doi.org/10.1016/J.PRECISIONENG.2024.08.004.
[11] A. Rahman, H. Jouini, N. Ghani, J.A. Rasani, H.A. Rahman, N. Jouini, J.A. Ghani, M. Rasidi, M. Rasani, A review of high-speed turning of AISI 4340 steel with minimum quantity lubrication (MQL), Coatings 14 (2024) 1063, https://doi.org/10.3390/COATINGS14081063.
[12] J.C. Lopes, A.G. Talon, M. de, S. Rodrigues, G.B. Moretti, F. de, C. Machado, G. G. de Souza, F.S.F. Ribeiro, L.E. de, A. Sanchez, E.C. Bianchi, An experimental evaluation between pure and diluted MQL versus flood lubri-cooling focused on cost and environmental impact, Int. J. Adv. Manufact. Technol. 129 (2023) 2691–2705, https://doi.org/10.1007/S00170-023-12399-6/FIGURES/12.
[13] E.C. Bianchi, R.L. Rodriguez, R.A. Hildebrandt, J.C. Lopes, H.J. de Mello, R.B. da Silva, P.R. de Aguiar, Plunge cylindrical grinding with the minimum quantity lubrication coolant technique assisted with wheel cleaning system, Int. J. Adv. Manuf. Technol. 95 (2018) 2907–2916, https://doi.org/10.1007/S00170-017-1396-5/METRICS.
[14] R. Arafat, G. Mahlfeld, K. Dröder, C. Herrmann, Towards cleaner machining: experimental investigation of collagen-in-water as a novel type of metalworking fluids – a technical feasibility study, J. Clean. Prod. (2024) 143987, https://doi.org/10.1016/J.JCLEPRO.2024.143987.
[15] P. Roy, J. De, S.B. Roy, S.K. Mazumder, M.K.S. Sarkar, Environmentally compliant materials and processes, Comprehens. Mater. Process. (2024) 40–57, https://doi.org/10.1016/B978-0-323-96020-5.00288-0.
[16] A. Elsheikh, A.B.M. Ali, A. Saba, H. Faqeha, A.A. Alsaati, A.M. Maghfuri, W. Abd-Elaziem, A.A. El Ashmawy, N. Ma, A review on sustainable machining: technological advancements, health and safety considerations, and related environmental impacts, Results Eng. 24 (2024) 103042, https://doi.org/10.1016/J.RINENG.2024.103042.
[17] R. Peng, L. Zhao, J. Tong, M. Chen, M. Zhou, A. Li, Design and evaluation of an internal-cooling grooved grinding wheel, J. Manuf. Process. 73 (2022) 1–16, https://doi.org/10.1016/J.JMAPRO.2021.10.061.
[18] R. Peng, J. Tong, X. Tang, X. Huang, K. Liu, Application of a pressurized internal cooling method in grinding inconel 718: Modeling-simulation and testing-validation, Int. J. Mech. Sci. 189 (2021), https://doi.org/10.1016/j.ijmecsci.2020.105985.
[19] J. Sieniawski, K. Nadolny, Experimental study into the grinding force in surface grinding of steel CrV12 utilizing a zonal centrifugal coolant provision system, Proc. Inst. Mech. Eng. B J. Eng. Manuf. 232 (2016) 394–403, https://doi.org/10.1177/0954405416645256.
[20] W. Stachurski, J. Sawicki, K. Krupanek, K. Nadolny, Application of numerical simulation to determine ability of air used in MQL method to clean grinding wheel active surface during sharpening of hob cutters, Int. J. Precis. Eng. Manufactur. - Green Technol. 8 (2021) 1095–1112, https://doi.org/10.1007/S40684-020-00239-X.
[21] Z. Guo, B. Guo, G. Wu, Y. Xiang, Q. Meng, J. Jia, Q. Zhao, K. Li, Z. Zeng, Three-dimensional topography modelling and grinding performance evaluating of micro-structured CVD diamond grinding wheel, Int. J. Mech. Sci. 244 (2023) 108079, https://doi.org/10.1016/J.IJMECSCI.2022.108079.
[22] H. Yu, K. Sun, W. Ren, J. Zhang, Z. Han, Synergistic improvement of grinding fluid utilization and workpiece surface quality using combinatorial bionic structured grinding wheels, J. Manuf. Process. 130 (2024) 102–117, https://doi.org/10.1016/J.JMAPRO.2024.08.046.
[23] Z. Chen, X. Zhang, D. Wen, S. Li, X. Wang, L. Gan, X. Rong, Improved grinding performance of SiC using an innovative bionic vein-like structured grinding wheel optimized by hydrodynamics, J. Manuf. Process. 101 (2023) 195–207, https://doi.org/10.1016/J.JMAPRO.2023.06.010.
[24] S.B. Thekkoot Surendran, V.S. Sooraj, Enhancing useful flow of cutting fluid and thermal performance in surface grinding via segmented wheel, Mater. Today Proc. 90 (2023) 208–213, https://doi.org/10.1016/J.MATPR.2023.06.090.
[25] A.S. Sobh, E.M. Sayed, A.F. Barakat, R.N. Elshaerr, Turning parameters optimization for TC21 Ti-alloy using Taguchi technique, Beni Suef Univ. J. Basic Appl. Sci. 12 (2023) 1–11, https://doi.org/10.1186/S43088-023-00356-X/FIGURES/6.
[26] M.W. Hisam, A.A. Dar, M.O. Elrasheed, M.S. Khan, R. Gera, I. Azad, The versatility of the Taguchi method: optimizing experiments across diverse disciplines, J. Statist. Theory Appl. (2024) 1–25, https://doi.org/10.1007/S44199-024-00093-9/FIGURES/4.
[27] H. Yu, W. Zhang, S. Zhang, J. Zhang, Z. Han, Optimization of hydrodynamic properties of structured grinding wheels based on combinatorial bionics, Tribol. Int. 173 (2022) 107651, https://doi.org/10.1016/J.TRIBOINT.2022.107651.
[28] X. Xiao, Y. Jin, R. Peng, S. Jiang, X. Huang, L. Zhao, J. Gao, J. Peng, Microscale viscous sintering model application to the preparation of metal bonded diamond grinding wheels, Int. J. Refract. Metals Hard Mater. 114 (2023) 106242, https://doi.org/10.1016/J.IJRMHM.2023.106242.
[29] M. Saeedipour, S. Vincent, J.L. Estivalezes, Toward a fully resolved volume of fluid simulation of the phase inversion problem, Acta Mech. 232 (2021) 2695–2714, https://doi.org/10.1007/S00707-021-02972-Z/FIGURES/21.
[30] A. Mohan, G. Tomar, Volume of fluid method: a brief review, J. Indian Inst. Sci. 104 (2024) 229–248, https://doi.org/10.1007/S41745-024-00424-W/FIGURES/15.
[31] A. Gupta, P. Swami, A.S.S. Balan, P. Kuppan, R. Oyyaravelu, Numerical modeling and heat transfer analysis of minimum quantity lubrication grinding of inconel 751, Mater. Today Proc. 5 (2018) 13358–13366, https://doi.org/10.1016/J.MATPR.2018.02.328.
[32] S. Mirjalili, A. Mani, A conservative second order phase field model for simulation of N-phase flows, J. Comput. Phys. 498 (2024) 112657, https://doi.org/10.1016/J.JCP.2023.112657.
[33] B. Sa, O. Klyus, V. Markov, V. Kamaltdinov, A numerical study of the effect of spiral counter grooves on a needle on flow turbulence in a diesel injector, Fuel 290 (2021) 120013, https://doi.org/10.1016/J.FUEL.2020.120013.
[34] S. Majumdar, S. Mandal, I. Biswas, D. Roy, S. Chakraborty, Modelling of air boundary layer around the grinding wheel, Int. J. Model. Simul. 40 (2020) 104–113, https://doi.org/10.1080/02286203.2018.1562013.
[35] M. Rasouli, S.M. Mousavi, H. Azargoshasb, O. Jamialahmadi, Y. Ajabshirchi, CFD simulation of fluid flow in a novel prototype radial mixed plug-flow reactor, J. Ind. Eng. Chem. 64 (2018) 124–133, https://doi.org/10.1016/J.JIEC.2018.03.008.
[36] A. Reid, R. Rossi, C. Cottini, A. Benassi, CFD simulation of a Rushton turbine stirred-tank using open-source software with critical evaluation of MRF-based rotation modeling, Meccanica (2024) 1–25, https://doi.org/10.1007/S11012-024-01824-Z/FIGURES/27.
[37] W. Kang, C. Meng, hao, J. Yu, R. Li, An dong, Numerical simulation of gas-liquid two-phase flow impacting fixed structure by CLSVOF/IB method based on OpenFOAM, J. Hydrodyn. 33 (2021) 1176–1189, https://doi.org/10.1007/S42241-021-0100-2/METRICS.
[38] F.M. White, Fluid Mechanics 7th Edition in SI units, (2016).
[39] S. Chakraborty, H.N. Datta, S. Chakraborty, Grey relational analysis-based optimization of machining processes: a comprehensive review, Process Integr. Optim. Sustainability 7 (2023) 609–639, https://doi.org/10.1007/S41660-023-00311-4/FIGURES/5.
[40] S. Costa, P. Capela, M.S. Souza, J.R. Gomes, L. Carvalho, M. Pereira, D. Soares, A new grinding wheel design with a 3D internal cooling structure system, J. Manufact. Mater. Process. 8 (2024) 159, https://doi.org/10.3390/JMMP8040159.
[41] S. Costa, P. Araújo, P. Capela, J. Gomes, J. Ribeiro, M. Pereira, D. Soares, Design of an experimental grinding machine for testing abrasive wheels with a 3D internal cooling channels structure, in: I. Alonso, A. Aranzabe, J. Barriga, A. Igartua (Eds.), Lubricants, Tribology and Condition Monitoring: LUBMAT-IBERTRIB 2024 Conference Program and Proceedings, Tekniker, San Sebastian, 2024, pp. 271–272.
[42] S.K. Tamil Vanan, E.U. Olugu, C.K. Ang, S.A. Lawal, O.C. Aja, Evaluation of surface grinding of AISI 304 stainless steel using dry and compressed air cooling techniques, SN Appl. Sci. 3 (2021) 1–10, https://doi.org/10.1007/S42452-021-04395-W/FIGURES/15.